Synthesis, Reactivity, and DFT Studies of S−C−S Zirconium(IV) Complexes

Thibault Cantat, Louis Ricard, Nicolas Mézailles, and Pascal Le Floch*

Laboratoire "Hétéroéléments et Coordination", Ecole Polytechnique, CNRS, Route de Saclay, 91128 Palaiseau, France

Received July 26, 2006

The reactivity of the bis(diphenylthiophosphinoyl) methanediide dianion **1** toward two Zr(IV) complexes was explored. Reaction of **1** with $[ZrCp_2Cl_2]$ cleanly yields the $[Zr(Cp_2)(SPPh_2CPPh_2S)]$ complex (**2**), in which the ligand behaves as a pincer ligand with two weak interactions between the ancillary sulfur ligands and the zirconium atom. Complex **2** is unreactive toward aldehydes and ketones. Reaction of **1** with $[ZrCl_4(THF)_2]$ affords a dimeric structure $[Zr(SPPh_2CPPh_2S)Cl_2(THF)]_2$ (**4**) in which two $[ZrCl_2(THF)(SPPh_2CPPh_2S)]$ units are bridged by the chloride ligands. Formation of **4** probably results from the dimerization of the $[Zr(SPPh_2CPPh_2S)Cl_2(THF)_2]$ complex (**3**), which was observed in the reaction mixture. The reaction of **4** with pyridine in excess affords $[Zr(SPPh_2CPPh_2S)Cl_2(py)_2]$ (**5**), which is a heptacoordinated complex in which both carbon and sulfur atoms of the $SPPh_2CPPh_2S^{2-}$ dianion are bound. The molecular structures of **2**, **4**, and **5** were determined by X-ray crystallography. Complexes **4** and **5** cleanly react with ketones ($R^1R^2C{=}O$) and aldehydes ($R^1HC{=}O$) to afford the corresponding geminal 1,1-bis(diphenylthiophosphinoyl) olefins of general formula $[(Ph_2P{=}S)C{=}C(R_1)(R_2)]$ and $[(Ph_2P{=}S)C{=}C(R_1)(H)]$. DFT calculations that were carried out on the model complex $[Zr(Cp_2)(SH_2P-C-PH_2S)]$ (**2t**) indicate that Zr−C bond only features a weak π-interaction between the carbon atom and a vacant orbital at the metal. Rotation of 90° yields complex **2t′**, which exhibits a stronger π-interaction, but this complex lies 30 kcal/mol higher in energy. Calculations on the model complex $[Zr(Cl)_2(py)_2(SH_2P-C-PH_2S)]$ (**5t**) yield the same conclusion regarding the weakness of π-bonding between the ligands and the zirconium fragment.

Introduction

Pincer ligands featuring an anionic carbon atom as central ligand have now widespread importance in coordination chemistry and catalysis.[1,2] In most cases, these pincer type structures, which can be regarded as equivalents of cyclopentadienyl ligands (L_2X, 6e donor ligands), feature two neighboring pendent arms ended by L-type heteroatomic ligands (O, N, P, S). However less attention has been paid so far to pincer systems that can act as eight-electron-donor ligands. Pioneering studies in this area were made by Cavell, who developed the use of mixed dianionic N−C−N **I** systems featuring a geminal dianionic carbon atom as central ligand.[3] These dianionic systems, which can be assembled through the metalation of bis(iminophosphoranyl)methane, proved to be very efficient in stabilizing various transition metal centers in different oxidation states, lanthanides, and aluminum as well.[4−7] Recently, we extended this approach to the synthesis of the hitherto unknown dianionic S−C−S pincer ligands **II**.[8] These new dianionic systems, which can be easily obtained through the double deprotonation of the methylene bridge of bis(diphenylthiophosphinoyl)methane, also bear an important potential in coordination chemistry (Chart 1). So far, Pd(II),[8] Ru(II),[9] Sm(III),[10] and Tm(III)[11] complexes were synthesized with this ligand.

Chart 1

I **II**

The coordination of a dianionic carbon center (4e donor) to an oxidized metal center led us to draw a double bond between the central carbon atom and the metal fragment. Although this formalism is commonly employed, early results on the electronic structure of electron-rich Pd(II) and Ru(II) complexes suggested that, in these species, the metal carbon bond bears a significant single-bond character and that an available lone pair remains on the carbon atom.[8,9] Interestingly, the nature of the metal−carbon bond in these complexes raises the general problem of the continuum that exists between coordinated geminal dianions and carbene complexes. The difference between the two forms

* Corresponding author. Tel: +33 1 69 33 45 70. Fax: +33 1 69 33 39 90. E-mail: lefloch@poly.polytechnique.fr.

(1) Albrecht, M.; van Koten, G. *Angew. Chem., Int. Ed.* **2001**, *40*, 3750−3781.

(2) van der Boom, M. E.; Milstein, D. *Chem. Rev.* **2003**, *103*, 1759−1792.

(3) Kasani, A.; Babu, R. P. K.; McDonald, R.; Cavell, R. G. *Angew. Chem., Int. Ed.* **1999**, *38*, 1483−1484.

(4) Cavell, R. G.; Babu, R. P. K.; Aparna, K. *J. Organomet. Chem.* **2001**, *617*, 158−169.

(5) Jones, N. D.; Cavell, R. G. *J. Organomet. Chem.* **2005**, *690*, 5485−5496.

(6) Smurnyy, Y.; Bibal, C.; Pink, M.; Caulton, K. G. *Organometallics* **2005**, *24*, 3849−3855.

(7) Cadierno, V.; Diez, J.; Garcia-Alvarez, J.; Gimeno, J.; Calhorda, M. J.; Veiros, L. F. *Organometallics* **2004**, *23*, 2421−2433.

(8) Cantat, T.; Mézailles, N.; Ricard, L.; Jean, Y.; Le Floch, P. *Angew. Chem., Int. Ed.* **2004**, *43*, 6382−6385.

(9) Cantat, T.; Demange, M.; Mézailles, N.; Ricard, L.; Jean, Y.; Le Floch, P. *Organometallics* **2005**, *24*, 4838−4841.

(10) Cantat, T.; Jaroschik, F.; Nief, F.; Ricard, L.; Mézailles, N.; Le Floch, P. *Chem. Commun.* **2005**, 5178−5180.

(11) Cantat, T.; Jaroschik, F.; Ricard, L.; Le Floch, P.; Nief, F.; Mézailles, N. *Organometallics* **2006**, *25*, 1329−1332.

10.1021/om060665v CCC: $33.50
Publication on Web 11/15/2006

Scheme 1

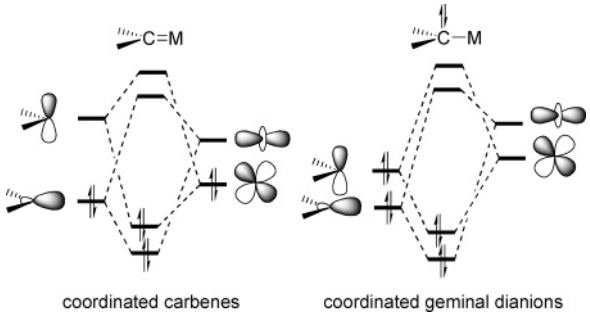

Scheme 2

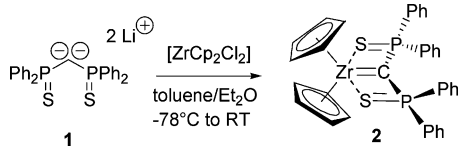

can be rationalized if one considers the simplified MO schemes in Scheme 1. In carbene complexes, it is assumed that donation occurs through the lone pair at carbon and that a π-back-donation develops between a filled metal orbital and the empty 2p orbital at carbon. In geminal dianions, two electrons are given through a first lone pair at carbon (sp^2 hybridized) and a second lone pair (2p) may also participate in the bonding via the overlap with an empty d orbital of appropriate symmetry at the metal. In this latter case, the double-bond character of the metal−carbon bond will therefore depend on the magnitude of this second contribution.

As part of a program aimed at investigating the synthetic potential of these S−C−S dianions, we recently explored the chemistry of d^0 Zr(IV)-based complexes. Herein we wish to report on their synthesis, their reactivity, and a complete DFT study that rationalizes their electronic structure.

Results and Discussion

Synthesis, X-ray Crystal Structures, and Reactivity of Complexes 2, 4, and 5. All our experiments were conducted with the readily available dianion **1**, which was generated by reacting 2 equiv of methyllithium with bis(diphenylthiophosphinoyl)methane in a toluene/ether (5:1) mixture.[8] Two metallic Zr(IV) fragments were chosen for this study, the well-known dichlorozirconocene and the $[ZrCl_4(THF)_2]$ complex. Dianion **1** reacts with $[ZrCp_2Cl_2]$ to yield complex **2**, which was isolated as a moisture-sensitive yellow solid in very good yield (Scheme 2). The coordination of the dianions in **2** affords a small upfield shift of the ^{31}P NMR resonance, which appears as a singlet at $\delta(CH_2Cl_2) = 20.9$ ppm compared to 24.5 in **1**. The symmetrical structure of **2** was confirmed by ^1H and ^{13}C NMR data. Interestingly, the carbon atom of the S−C−S ligand resonates at very high field ($\delta = 33.0$ ppm; $^1J_{PC} = 86.1$ Hz) compared to those usually recorded for classical Zr carbene complexes (230−300 ppm), thus suggesting that this atom bears a substantial negative charge.[12−17] This chemical shift is also much more shielded than in the bis(iminophosphorane) methanediide Zr complex $[ZrCl_2\{C(Me_3Si{=}NPPh_2)_2\text{-}\kappa^3C,N,N\}]$ ($\delta = 101.7$ ppm).[18]

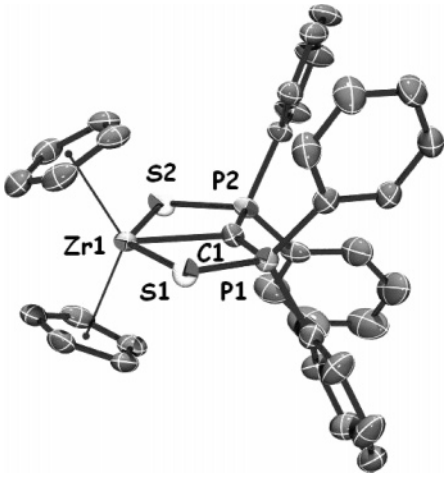

Figure 1. Molecular structure of complex **2**. Thermal ellipsoids are drawn at the 50% probability level. Hydrogen atoms are omitted for clarity. Selected bond distances (Å) and angles (deg): Zr1−C1 2.251(2), Zr1−S1 2.7499(6), P1−S1 2.019(1), P2−S2 2.010(8), P1−C1 1.670(2), P2−C1 1.666(2), P1−C1−P2 145.7(1), Zr1−C1−P1 106.4(1),Zr1−C1−P2107.8(1).

Definitive evidence of the binding mode of **1** in **2** was provided by an X-ray diffraction analysis. Single crystals of **2** were obtained by slowly diffusing hexanes (mixture of isomers) on a dichloromethane solution of the complex at room temperature. A view of one molecule of **2** is presented in Figure 1, and the most relevant bond distances and angles are listed in the corresponding legend. Crystal data and structure refinement details are given in Table 1. Complex **2** can be described, at first sight, as a 20 VE complex, the S−C−S ligand acting as 8e donor ligand through the carbon atom (4e) and the two sulfur atoms (2e for each), but further calculations will show that the electronic situation is much more subtle. The most significant structural feature of **2** is the planar S(1)−P(1)−C(1)−P(2)−S(2) core. At 2.251(2) Å the Zr(1)−C(1) bond is significantly longer than the corresponding Zr=C bond in $[Zr(CH_2Ph)_2\{C(Ad{-}N{=}PPh_2)_2\}\text{-}\kappa^3C,N,N]$ (Ad = adamantyl) (2.208(3) Å).[19] At 1.668 Å (av), the P−C bonds are short, as short as in the isolated dianion **1** (1.681 Å (av)).[20] This suggests a participation of the thiophosphinoyl arms in the stabilization of an important electron density on the carbon atom via negative hyperconjugation. According to these data, the Zr−C π-interaction must be weak and **2** may also be described as a 18 VE complex with a remaining lone pair on the carbon center. The two Zr−S interatomic distances of 2.7499(6) and 2.7679(6) Å are rather long, consistent with a weak dative interaction. These Zr−S distances are 0.3−0.4 Å longer than the corresponding average Pd−S and Ru−S distances of 2.371 and 2.479 Å observed in $[Pd(PPh_3)(SPPh_2CPPh_2S)]$ and $[Ru(PPh_3)_2(SPPh_2CPPh_2S)]$, respectively.[8,9]

(12) Clift, S. M.; Schwartz, J. *J. Am. Chem. Soc.* **1984**, *106*, 8300−8301.
(13) Barger, P. T.; Santarsiero, B. D.; Armantrout, J.; Bercaw, J. E. *J. Am. Chem. Soc.* **1984**, *106*, 5178−5186.
(14) Fryzuk, M. D.; Mao, S. S. H.; Zaworotko, M. J.; Macgillivray, L. R. *J. Am. Chem. Soc.* **1993**, *115*, 5336−5337.
(15) Hartner, F. W.; Schwartz, J.; Clift, S. M. *J. Am. Chem. Soc.* **1983**, *105*, 640−641.
(16) Schwartz, J.; Gell, K. I. *J. Organomet. Chem.* **1980**, *184*, C1−C2.
(17) Beckhaus, R. *Angew. Chem., Int. Ed. Engl.* **1997**, *36*, 687−713.
(18) Cavell, R. G.; Babu, R. P. K.; Kasani, A.; McDonald, R. *J. Am. Chem. Soc.* **1999**, *121*, 5805−5806.
(19) For comparison, a search performed on the Cambridge Structural Database afforded six zirconium alkylidene complexes: we found an average Zr−C bond length of 2.141 Å (median 2.156 Å). 620 structures were found for Zr−alkyl complexes (average 2.381 Å, median 2.349 Å) and 187 structures for Zr−vinyl complexes (average 2.274 Å, median 2.261 Å).
(20) Cantat, T.; Ricard, L.; Le Floch, P.; Mézailles, N. *Organometallics* **2006**, *25*, 4965−4976.

Table 1. Crystal Data and Structural Refinement Details for Structure of Complexes 2, 4, and 5

	2	4	5
cryst size [mm]	0.22 × 0.22 × 0.16	0.22 × 0.20 × 0.12	0.22 × 0.18 × 0.18
empirical formula	$C_{35}H_{30}P_2S_2Zr,2/3(C_7H_8)$	$C_{58}H_{56}Cl_4O_2P_4S_4Zr_2,5(C_7H_8)$	$C_{35}H_{30}Cl_2N_2P_2S_2Zr$
molecular weight	729.29	1822.10	766.79
cryst syst	monoclinic	monoclinic	monoclinic
space group	*C*2/*c*	$P2_1/c$	$P2_1/c$
a [Å]	18.033(1)	19.651(1)	14.290(1)
b [Å]	15.609(1)	13.107(1)	13.699(1)
c [Å]	38.393(2)	17.849(1)	17.819(1)
α [deg]	90.00	90.00	90.00
β [deg]	102.405(1)	104.408(1)	94.419(1)
γ [deg]	90.00	90.00	90.00
V [Å]^3	10554.4(10)	4452.7(5)	3477.9(4)
Z	12	2	4
calcd density [g·cm^{-3}]	1.377	1.359	1.464
abs coeff [cm^{-1}]	0.549	0.567	0.710
θ_{max} [deg]	30.03	27.48	30.03
F(000)	4504	1884	1560
index ranges	−25 25; −17 21; −54 54	−25 25; −15 17; −18 17	−20 20; −19 17; −25 25
no. of reflns collected/indep	15 543/11 847	15 737/9318	17 717/10 043
no. of reflns used	9286	7437	7879
(R_{int})	0.0156	0.0292	0.0326
no. of params refined	606	526	397
refln/param	15	14	19
final R1[a]/wR2 [$I > 2\sigma(I)$][b]	0.0378/0.1015	0.0483/0.1414	0.0398/0.1151
goodness-of-fit on F^2	1.061	1.033	1.053
diff peak/hole [e·Å^{-3}]	0.700(0.063)/−0.662(0.063)	1.001(0.083)/−0.942(0.083)	1.333(0.085)/ −0.923(0.085)

[a] $R1 = \sum||F_o| - |F_c||/\sum|F_o|$. [b] $wR2 = (\sum w||F_o| - |F_c||^2/\sum w|F_o|^2)^{1/2}$.

Scheme 3

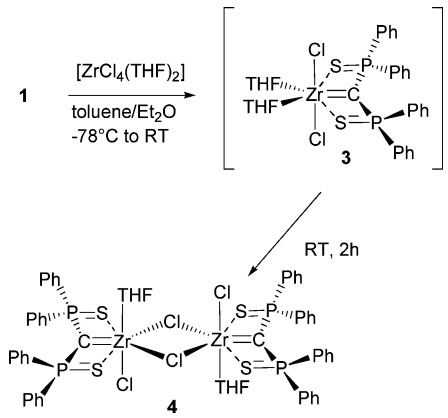

Dianion **1** reacted with $[ZrCl_4(THF)_2]$ to afford complex **3**, which adopts a symmetrical structure on the basis of the appearance of a singlet at $\delta = 16.3$ ppm in the ^{31}P NMR spectrum. Complex **3** is converted within 2 h to complex **4**, as evidenced by a downfield shift of the ^{31}P resonance to 20.3 ppm. Complex **4** was isolated as a moisture-sensitive yellow solid and fully characterized using conventional NMR techniques (Scheme 3). Its ^{13}C NMR spectrum displays a characteristic triplet at $\delta = 100.8$ ppm ($^1J_{PC} = 81.7$ Hz). This value markedly differs from that recorded for complex **2** and is closer to that reported for $[ZrCl_2\{C(Me_3Si{=}NPPh_2)_2\text{-}\kappa^3C,N,N\}]$ and those of ylide complexes of zirconium.[21]

An X-ray crystal structure analysis was carried out. Single crystals of **4** were grown at room temperature by diffusing hexanes into a dichloromethane solution of the complex. The structure of **4** is presented in Figure 2, and the most significant metric parameters are presented in the corresponding legend. Crystal data and structure refinement details are given in Table 1. Compound **4** adopts a dimeric structure where two chloride ligands bridge two [ZrCl(THF)(**1**)] units. Therefore, although

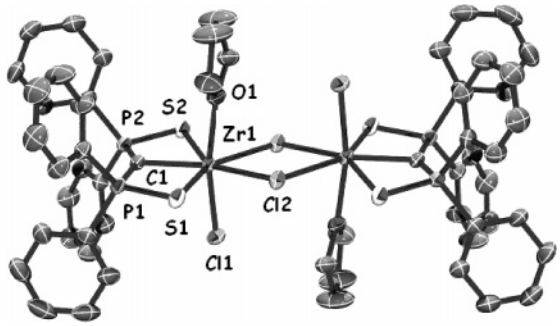

Figure 2. Molecular structure of complex **4**. Thermal ellipsoids are drawn at the 50% probability level. Hydrogen atoms are omitted for clarity. Selected bond distances (Å) and angles (deg): Zr1−C1 2.180(3), Zr1−S1 2.6813(8), Zr1−S2 2.6912(8), P1−S1 2.025(1), P2−S2 2.020(1), P1−C1 1.677(3), P2−C1 1.674(3), P1−C1−P2 144.8(2), Zr1−C1−P1 107.5(1), Zr1−C1−P2 107.2(1).

no further characterization could be carried out due to its poor stability in solution, complex **3** was assumed to be a monomeric form featuring two molecules of THF as ligand.

Contrary to bis(iminophosphorane) methanediide Zr(IV) complexes, **4** adopts a dimeric structure in the solid state.[18,22,23] Very probably, this dimerization does not result from a particular electronic situation in ligand **1** but rather from the absence of steric crowding on the two thiophosphinoyl ligands with regard to the nitrogen derivative, which possesses Me_3Si or adamantyl substituents. The Zr−C bond distance of 2.180(3) Å in **4** is similar to that reported by Cavell for the Zr−C distance of 2.208(3) Å in $[Zr\{C(Ad{=}NPPh_2)_2\text{-}\kappa^3C,N,N\}(CH_2Ph)_2]$. In contrast, the Zr−S distances are ca. 0.1 Å shorter than those observed in **2**. Upon addition of excess pyridine, complex **4** is cleanly converted to **5**, which was isolated as a yellow moisture-sensitive solid (Scheme 4).

(21) Cavell, R. G.; Babu, R. P. K.; Kasani, A.; McDonald, R. *J. Am. Chem. Soc.* **1999**, *121*, 5805−5806, and references therein.

(22) Babu, R. P. K.; McDonald, R.; Decker, S. A.; Klobukowski, M.; Cavell, R. G. *Organometallics* **1999**, *18*, 4226−4229.

(23) Aparna, K.; Babu, R. P. K.; McDonald, R.; Cavell, R. G. *Angew. Chem., Int. Ed.* **2001**, *40*, 4400−4402.

Scheme 4

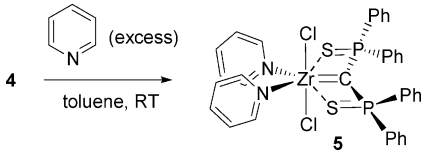

Interestingly, although the formation of **5** is not accompanied by a significant shift in ^{31}P NMR spectroscopy (from 24.5 ppm in **1** to 22.9 ppm in **5**), we note, like in **4**, a significant downfield shift of the ^{13}C NMR chemical shift of the central carbon atom ($\delta(CD_2Cl_2) = 97.0$ ppm with $^1J_{CP} = 83.1$ Hz), thus confirming the idea that the electronic situation in **4** and **5** probably differs from that in **2**. A view of one molecule of **5** is presented in Figure 3, and the most significant bond distances and angles are listed in the corresponding legend. Crystal data and structure refinement details are given in Table 1.

Having in hand these three Zr(IV) complexes, their reactivity was then studied. Although the reactivity of monodentate M(IV)═C(R_2) (M = group 4 metal) is well documented,[12,24,25] that of polydentate derivatives has not been widely explored.[10,11] In 2000, Cavell and his group reported on the successful [2+2] cycloadditions of heteroallenes (CO_2, isonitiles, carbodiimides) on the C═M bond of bis(iminophosphorane) methanediide complexes of Hf and Zr.[26] Like in the case of lanthanide (Sm, Tm) derivatives, whose structures and chemistry were reported recently, we explored the reactivity of **2**−**5** toward aldehydes and ketones. Surprisingly, complex **2** proved to be unreactive toward these electrophiles. This lack of reactivity can probably be ascribed to the electronic saturation (formally 20 VE) and the steric crowding around the zirconium center, which precludes coordination of the oxygen atom. On the contrary, complexes **4** and **5** were found to be highly reactive toward aldehydes, affording the corresponding geminal bis(diphenylthiophosphinoyl) olefins. Compounds **6** and **7** were isolated in very good yields as very stable yellow powders after a conventional workup and chromatographic purification. Complexes **4** and **5** also react with ketones in dichloromethane at 40 °C to afford compounds **8**, **9**, and **10**, which were successfully characterized by NMR spectroscopy and elemental analyses (Scheme 5).

DFT Calculations on the Electronic Structure of Complexes 2 and 5. DFT calculations were carried out to shed some light on the electronic structures of complexes **2** and **5**. The Gaussian 03 set of programs was used for this study.[27] Optimizations were not conducted on the real molecules but

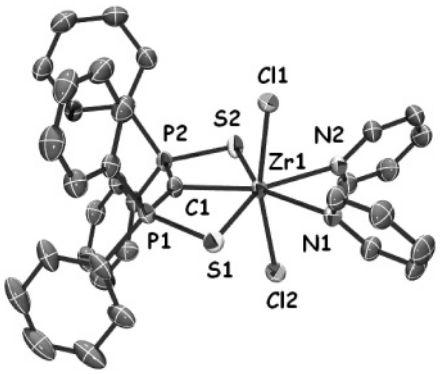

Figure 3. Molecular structure of complex **5**. Thermal ellipsoids are drawn at the 50% probability level. Hydrogen atoms are omitted for clarity. Selected bond distances (Å) and angles (deg): Zr1−C1 2.172(2), Zr1−S1 2.7064(5), Zr1−S2 2.6714(5), P1−S1 2.0241(7), P2−S2 2.0219(7), P1−C1 1.678(2), P2−C1 1.676(2), P1−C1−P2 145.7(1), Zr1−C1−P1 107.2(1), Zr1−C1−P2 107.1(1).

Scheme 5

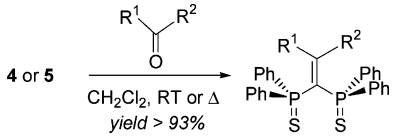

6: R^1 = H, R^2 = 9-anthracenyl
7: R^1 = H, R^2 = 2-furyl
8: $R^1 = R^2$ = Ph
9: $R^1 = R^2$ = 2-pyridyl
10: $R^1 = R^2$ = 2-thienyl

Scheme 6

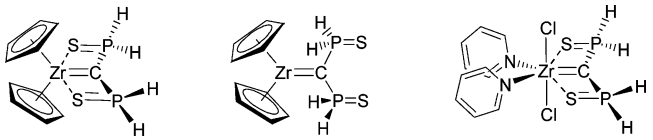

on models **2t**, **2t′**, and **5t** (t meaning theoretical) in which the phenyl groups at phosphorus were replaced by hydrogen atoms (see Scheme 2). Details of these calculations (methods, functional, and basis sets employed) are presented in the Experimental Section.

The MO representation of the π-interaction of **2t** is presented in Figure 4. Examination of metric parameters reveals a very good agreement with experimental data. The Zr(1)−C(1) bond at 2.263 Å and the P−C (1.684 Å) and the P−S bonds (2.041 Å) are very close to the experimental values. Only the Zr−S bonds were found to be ca. 0.1 Å longer than in the experimental structure (2.873 Å). To analyze the Zr═C double bond character in **2t**, a MO diagram describing the π-interactions was built by decomposing the complex into two fragments, the dianionic ligand **1** (fragment a) and the [Cp_2Zr^{2+}] fragment (fragment b) (Figure 4). Interactions between the two fragments were analyzed using the AOMIX program developed by Gorelsky.[28,29] As can be seen, π-interactions in **2t** mainly result from the combination of four FO (fragment orbitals). In fragment a the two orbitals involved are the HOFOa-4, which is the bonding combination of lone pairs at the central carbon atom and one lone pair at each sulfur atom, and the HOFOa-1, which is the

(24) Beckhaus, R.; Santamaria, C. *J. Organomet. Chem.* **2001**, *617*, 81−97.
(25) Tebbe, F. N.; Parshall, G. W.; Reddy, G. S. *J. Am. Chem. Soc.* **1978**, *100*, 3611−3613.
(26) Babu, R. P. K.; McDonald, R.; Cavell, R. G. *Organometallics* **2000**, *19*, 3462−3465.
(27) Frisch, M. J.; Trucks, G. W.; Schlegel, H. B.; Scuseria, G. E.; Robb, M. A.; Cheeseman, J. R.; Montgomery, J. A., Jr.; Vreven, T.; Kudin, K. N.; Burant, J. C.; Millam, J. M.; Iyengar, S. S.; Tomasi, J.; Barone, V.; Mennucci, B.; Cossi, M.; Scalmani, G.; Rega, N.; Petersson, G. A.; Nakatsuji, H.; Hada, M.; Ehara, M.; Toyota, K.; Fukuda, R.; Hasegawa, J.; Ishida, M.; Nakajima, T.; Honda, Y.; Kitao, O.; Nakai, H.; Klene, M.; Li, X.; Knox, J. E.; Hratchian, H. P.; Cross, J. B.; Bakken, V.; Adamo, C.; Jaramillo, J.; Gomperts, R.; Stratmann, R. E.; Yazyev, O.; Austin, A. J.; Cammi, R.; Pomelli, C.; Ochterski, J. W.; Ayala, P. Y.; Morokuma, K.; Voth, G. A.; Salvador, P.; Dannenberg, J. J.; Zakrzewski, V. G.; Dapprich, S.; Daniels, A. D.; Strain, M. C.; Farkas, O.; Malick, D. K.; Rabuck, A. D.; Raghavachari, K.; Foresman, J. B.; Ortiz, J. V.; Cui, Q.; Baboul, A. G.; Clifford, S.; Cioslowski, J.; Stefanov, B. B.; Liu, G.; Liashenko, A.; Piskorz, P.; Komaromi, I.; Martin, R. L.; Fox, D. J.; Keith, T.; Al-Laham, M. A.; Peng, C. Y.; Nanayakkara, A.; Challacombe, M.; Gill, P. M. W.; Johnson, B.; Chen, W.; Wong, M. W.; Gonzalez, C.; Pople, J. A. *Gaussian 03*, revision C.02; Gaussian, Inc.: Wallingford, CT, 2004.
(28) Gorelsky, S. I. *AOMix: Program for Molecular Orbital Analysis*; York University: Toronto, Canada, 1997; http://www.sg-chem.net/.
(29) Gorelsky, S. I.; Lever, A. B. P. *J. Organomet. Chem.* **2001**, *635*, 187−196.

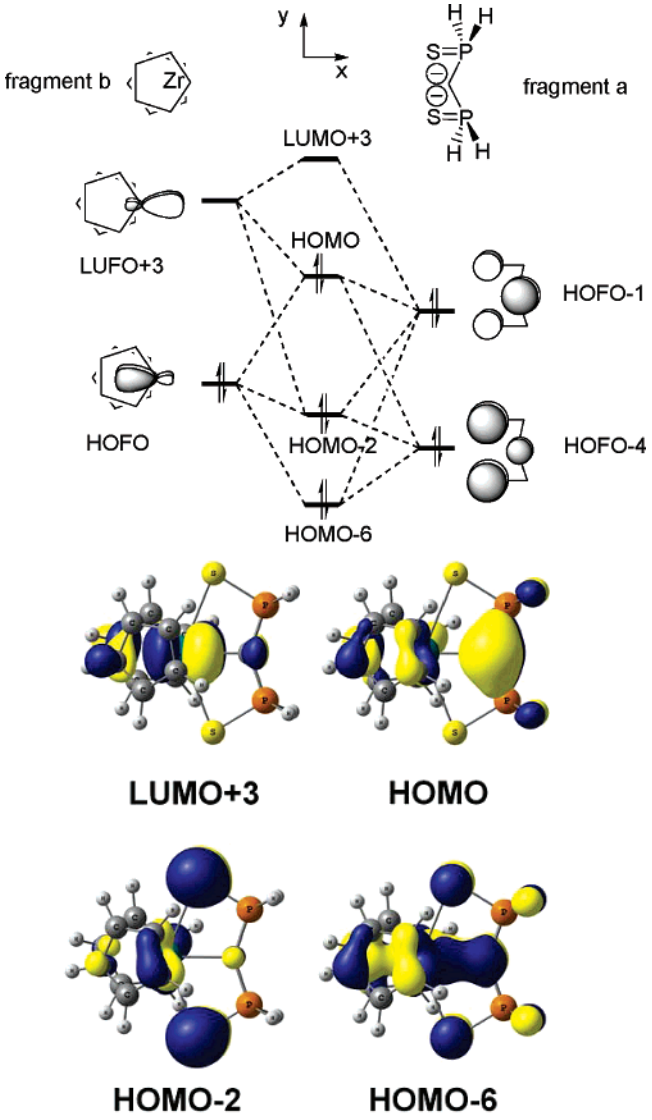

Figure 4. Simplified MO diagram of the π-interaction in **2t** between ligand **1** (modelized by fragment a) and the zirconocene [Cp_2Zr^{2+}] fragment (fragment b).

corresponding antibonding orbital. In fragment b, two hybrid orbitals that involve the d_{xz} metal orbital participate in the bonding: The LUFOb+3, which is polarized in the direction of fragment a, and the HOFOb, which features an important contribution of the d_{xz} metal orbital. This orbital is also bonding with the Cp ligands. The Zr=C π-bond character, which results from the donation of the carbon $2p_z$ lone pair to the metal, can be quantified by the participation of the metal fragment vacant orbitals in the occupied MOs of the π-interaction diagram. In **2t**, this electronic transfer involves the unoccupied LUFOb+3. Participation of this fragment orbital is weak since it reaches 10.0% in the HOMO and only 1.1% in the HOMO-2 (0.0% in HOMO-6). Therefore, an important electron density remains on the carbon atom (see HOMO, Figure 4).

Another interesting point concerns the geometry and the electron counting in complex **2t**. Indeed, one may wonder why ligand **1** is not oriented perpendicular to the equatorial plane bisecting the wedge defined by the Cp_2Zr fragment. Calculations carried out in this geometry showed that complex **2t′** lies at higher energy (+30.0 kcal/mol). Interestingly, in this conformation, the π-interaction seems to be more important than in complex **2t** and the Wiberg bond index is significantly increased (1.16 vs 0.69 in **2t**). In addition, the calculated Zr−C bond distance is reduced (2.120 vs 2.263 Å in **2t**). Examination of the molecular orbitals in **2t′** reveals that the π-interaction results from the overlap of the HOFOa ($2p_y$ orbital at carbon) and HOFOa-2 (mainly lone pairs at S) with the LUFOb+1 (d_{xy} orbital at zirconium), as shown in Figure 5. Analysis of the different contributions indicate that the HOMO features a very important contribution of the HOFOa-2 (61.1%), a modest contribution of the HOFOa (22.7%), and a weak contribution of the LUFOb+1 metal orbital (11.1%). Therefore this MO mainly describes a combination of the two available lone pairs at the sulfur atoms and features only a weak zirconium−carbon bond character. The Zr=C π-bond character in **2t′** is mainly described by the HOMO-4, to which the LUFOb+1 vacant orbital contributes at 20.4% (Figure 5). This results in a greater donation of the carbon 2p lone pair to the metal in **2t′** ($\sum$%(LUFOb+1) = 31.5% in the occupied MOs) than in **2t** ($\sum$%(LUFOb+3) = 11.1% in the occupied MOs). This difference arises from the energetic gap that separates these two acceptor fragment orbitals (ΔE(LUFOb+1/LUFOb+3) = 1.8 eV). We conclude that the preference for the conformation **2t** most likely results from the σ-bonding scheme: the d^0 Cp_2Zr^{2+} fragment is able to accommodate three ligands in the bent-metallocene plane,[30] so that coordination of the sulfur atoms is favored even if the Zr=C π-bond is weakened.

The results of the DFT computations suggest that complex **2** cannot be viewed as a real 20 VE complex. The most satisfying description is to consider that **2** is a 18 VE complex in which only six electrons are given by ligand **1**, two electrons being localized in a lone pair at the central carbon atom. On the other hand, the participation of the σ^*_{PH} antibonding orbitals in the stabilization of this lone pair is reflected by the presence of short P−C bond distances (with low Wiberg indexes at 1.08).[20,31,32]

The optimized structure of complex **5t** was also found to be very close to that obtained for the real complex **5** by X-ray diffraction analysis. The shortening of the Zr−C bond with regard to **2** is well reproduced (2.199 Å in **5t** vs 2.172(2) Å in **5**) as well as the variation of the P−C bonds (1.676(2) Å in **5** vs 1.687 Å in **5t**). Even the difference in the Zr−S bond lengths is relatively weak (2.7064(5) Å in **5** vs 2.771 Å in **5t**). The electronic structure of **5t** is close to that of complex **2t**, as can be viewed in the MO diagram in Figure 6. The HOFOa-1 and HOFOa-4 interact with the vacant LUFOb+2 metal orbital. The HOMO and the HOMO-2, which describe the π-interaction in **5t**, feature an important contribution of the ligand and only a weak contribution of the metal orbital. Thus, contributions of these three orbitals in the HOMO are the following: 8.8% LUFOb+2, 85.1% HOFOa-1, and 2.9% HOFOa-4. The HOMO-2 mainly consists of a combination of the HOFOa-4 (76.3%) and the LUFOb+2 (5.1%). Therefore if we sum the contribution of the vacant d_{xz} in complexes **2t** and **5t**, it appears that the π-bonding is slightly more important in the latter (11% in **2t** vs 13% in **5t**). This comparison is confirmed by the value of the Wiberg bond of the Zr−C bond index in **5t** (0.80 vs 0.69 in **2t**).

Analyses of the electronic structures of complexes **2t** and **5t** reveal that the carbon−metal bond has a low double-bond character and a low bond order. In the free geminal dianion,

(30) Lauher, J. W.; Hoffmann, R. *J. Am. Chem. Soc.* **1976**, *98*, 1729−1742.
(31) Reed, A. E.; Curtiss, L. A.; Weinhold, F. *Chem. Rev.* **1988**, *88*, 899−926.
(32) Reed, A. E.; Schleyer, P. V. *J. Am. Chem. Soc.* **1990**, *112*, 1434−1445.

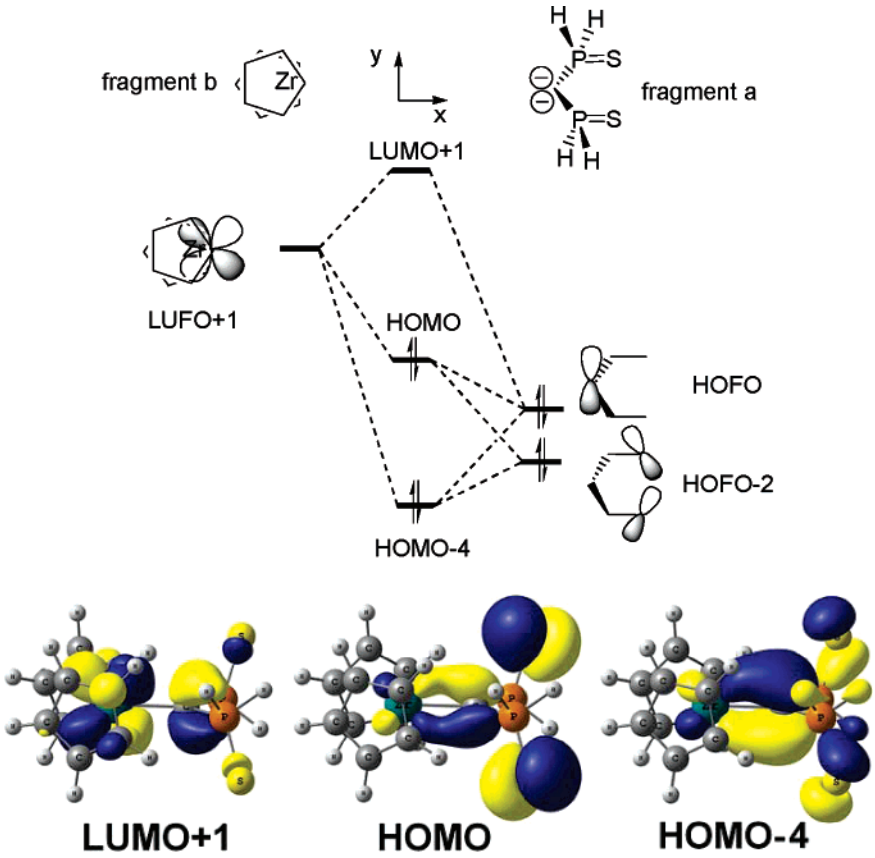

Figure 5. Simplified MO diagram of the π-interaction between dianionic ligand **1** (modelized by fragment a) and the zirconocene [Cp_2Zr^{2+}] fragment (fragment b) in complex **2t′**.

the electron-withdrawing groups (EWG) strongly stabilize the two carbon lone pairs by negative hyperconjugation (short PC bonds with low bond orders).[20,31,32] In the corresponding complexes, the same stabilization occurs so that the carbon p_π orbital is low in energy. This lone pair at carbon can overlap with a metal orbital of appropriate symmetry. This π-donation, responsible for the double-bond character, is weak in **2** and **5**. For comparison, in Fischer-type carbene complexes, the metal−carbene bond can be described by donor/acceptor interactions. The σ-donation from the carbene lone pair to a metal orbital accounts for the σ-bond and the π-interaction results from the π-back-donation from the occupied d_{xz} metal orbital into the vacant p_π orbital at carbon, the latter being stabilized by electron-donating groups (EDG) (bonding scheme A in Scheme 7).[33] In Schrock-type complexes the carbene center usually possesses alkyl substituents and the metal−carbene bond is best described by the interaction between two triplet fragments (bonding scheme B in Scheme 7).[33] For coordinated dianions, the metal carbon interaction results from σ- and π-donation from the two carbon lone pairs to the metal (bonding scheme C in Scheme 7). The two EWG polarize the double bond so that the carbon atom still bears an important negative charge and exhibits a nucleophilic character.

Conclusion

In conclusion, we have shown in this paper that Zr(IV) complexes of the dianionic ligand **1** are available through simple metathesis of the chloride ligands in [$ZrCp_2Cl_2$] and [$Zr(THF)_2Cl_4$] complexes. Whereas the Cp derivative ([$ZrCp_2(SPPh_2CPPh_2S)$], **2**) proved to be unreactive toward ketones and aldehydes, complex [$Zr(py)_2Cl_2(SPPh_2CPPh_2S)$] (**5**) proved to be an efficient precursor of geminal 1,1-bis(diphenylthiophosphinoyl) olefins. Coordination of dianion **1** toward the Zr(IV) center involves both σ- and π-donation of the dianion lone pairs to the metal vacant orbitals. DFT calculations revealed that, in complexes **2** and **5**, the double-bond character is weak and the formal π-bond is strongly polarized toward the carbon atom. This particular bonding scheme results from the presence of two electron-withdrawing thiophosphinoyl arms that are able to stabilize a lone pair of π-symmetry on the carbon via negative hyperconjugation. An interesting goal would now consist in exploiting the reactivity of the remaining lone pair at carbon to promote catalytic transformations. Studies aimed at validating this hypothesis are currently under active investigation in our laboratory.

Experimental Section

General Remarks. All reactions were routinely performed under an inert atmosphere of argon or nitrogen by using Schlenk and glovebox techniques and dry deoxygenated solvents. Dry THF, ether, and hexanes were obtained by distillation from Na/benzophenone. Dry dichloromethane was distilled on P_2O_5 and dry toluene on Na. Nuclear magnetic resonance spectra were recorded on a Bruker AC-300 SY spectrometer operating at 300.0 MHz for ^{1}H, 75.5 MHz for ^{13}C, and 121.5 MHz for ^{31}P. Solvent peaks are used as internal reference relative to Me_4Si for ^{1}H and ^{13}C chemical shifts (ppm); ^{31}P chemical shifts are relative to a 85% H_3PO_4 external reference. Coupling constants are given in hertz. The following abbreviations are used: s, singlet; d, doublet; t, triplet; m, multiplet; v, virtual. Elemental analyses were performed by the "Service d'analyse du CNRS", at Gif sur Yvette, France. Bis(diphenylthio-

(33) Vyboishchikov, S. F.; Frenking, G. *Chem.−Eur. J.* **1998**, *4*, 1428−1438.

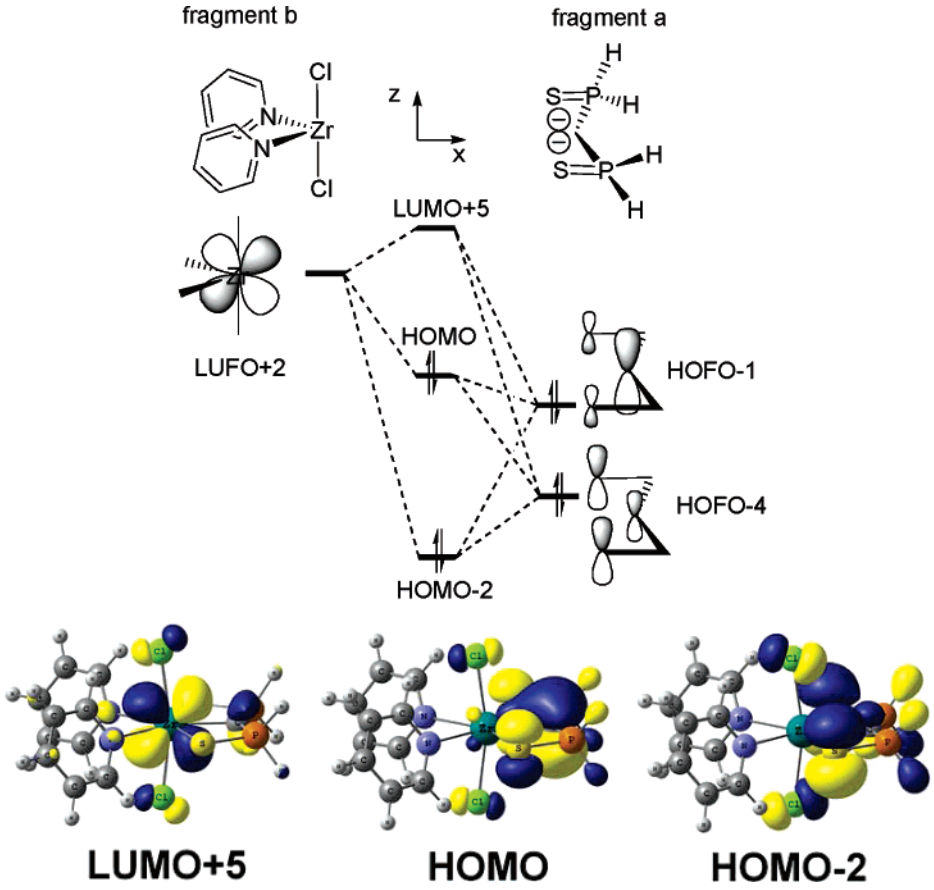

Figure 6. Simplified MO diagram of the π-interaction between dianionic ligand **1** (modelized by fragment a) and the $[ZrCl_2(py)_2^{2+}]$ fragment (fragment b) in complex **5t**.

Scheme 7

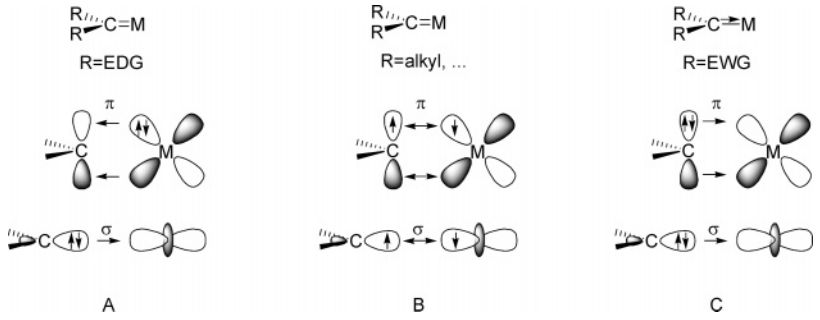

phosphinoyl)methane and the bis(diphenylthiophosphinoyl) methanediide lithium salt were prepared according to literature procedures.[8,34] All other reagents and chemicals were obtained commercially and used as received.

Synthesis of Complex 2. One equivalent of Cp_2ZrCl_2 (195 mg, 0.67 mmol) was added to a solution of dianion **1** in toluene (5.0 mL, 0.13 mol/L, 0.67 mmol) at room temperature. ^{31}P NMR spectroscopy showed the reaction to be complete. LiCl salt was eliminated via centrifugation after addition of 10 mL of dichloromethane. Pure complex **2** was finally isolated as a yellow solid after evaporation of the solvents (98% yield, 437 mg). Selected data: ^1H NMR (300 MHz, CD_2Cl_2, 25 °C, CD_2Cl_2 δ = 5.62 ppm as internal reference) δ 6.15 (s, 10H; Cp-*H*), 7.25 (m, 8H; phenyl-H_{meta}), 7.40 ppm (m, 12H; phenyl-H_{ortho} + H_{para}); $^{13}C\{^1H\}$ NMR (75.465 MHz, CD_2Cl_2, 25 °C, CD_2Cl_2 δ = 54.0 ppm as internal reference) δ 32.8 (t, $^1J_{PC}$ = 86.2 Hz; P*C*P), 113.0 (s; Cp-*C*), 128.6 (d, $^3J_{PC}$ = 12.7 Hz; phenyl-C_{meta}), 130.6 (s; phenyl-C_{para}), 130.7 (d, $^2J_{PC}$ = 12.4 Hz; phenyl-C_{ortho}), 139.8 ppm (dd, $^1J_{PC}$ = 73.0 Hz, $^3J_{PC}$ = 1.6 Hz; phenyl-C_{ipso}); $^{31}P\{^1H\}$ NMR (121.5 MHz, CD_2Cl_2, 25 °C, 85% H_3PO_4 as external standard) δ 21.2 ppm (s). Anal. Calcd for $C_{35}H_{30}P_2S_2Zr$: C, 62.94; H, 4.53; Found: C, 62.63; H, 4.41.

Synthesis of Complex 4. One equivalent of $ZrCl_4(THF)_2$ (150 mg, 0.40 mmol) was added to a solution of dianion **1** in toluene (3.0 mL, 0.13 mol/L, 0.40 mmol) at room temperature. The solution was stirred 2 h at room temperature. The resulting solid was isolated by centrifugation and complex **4** extracted with dichloromethane (10 mL). Pure complex **4** was finally isolated as a yellow solid after evaporation of the solvents (91% yield, 248 mg). Selected data: ^1H NMR (300 MHz, CD_2Cl_2, 25 °C, CD_2Cl_2 δ = 5.62 ppm as internal reference) δ 1.85 (m, 4H; THF), 3.82 (m, 4H; THF), 7.22 (m, 8H; phenyl-H_{meta}), 7.38 (m, 4H; phenyl-H_{para}), 7.47 ppm (m, 8H; phenyl-H_{ortho}); $^{13}C\{^1H\}$ NMR (75.465 MHz, CD_2Cl_2, 25 °C, CD_2Cl_2 δ = 54.0 ppm as internal reference) δ 26.1 (s; THF), 69.4 (s; THF), 100.8 (t, $^1J_{PC}$ = 81.7 Hz; P*C*P), 128.6 (d, $^2J_{PC}$ = 12.7 Hz; phenyl-C_{meta}), 131.3 (d, $^4J_{PC}$ = 2.4 Hz; phenyl-C_{para}), 131.5 (d, $^2J_{PC}$ = 12.4 Hz; phenyl-C_{ortho}), 136.2 ppm (d, $^1J_{PC}$ = 77.4 Hz;

(34) Grim, S. O.; Mitchell, J. D. *Inorg. Chem.* **1977**, *16*, 1762−1770.

phenyl-C_{ipso}); $^{31}P\{1H\}$ NMR (121.5 MHz, CD_2Cl_2, 25 °C, 85% H_3PO_4 as external standard) δ 20.3 ppm (s).

Synthesis of Complex 5. One equivalent of $ZrCl_4(THF)_2$ (150 mg, 0.40 mmol) was added to a solution of dianion **1** in toluene (3.0 mL, 0.13 mol/L, 0.40 mmol) at room temperature. Pyridine (0.3 mL) was then added. Evaporation of the solvents afforded a yellow solid, which was dissolved in dichloromethane. LiCl salt was eliminated via centrifugation after addition of 10 mL of dichloromethane. Pure complex **2** was finally isolated as a yellow solid after evaporation of the solvents (97% yield, 297 mg). A diffusion of hexanes (mixture of isomers) into a dichloromethane solution of **5** allowed the growth of single crystals for an X-ray diffraction study. Selected data: ^1H NMR (300 MHz, CD_2Cl_2, 25 °C, CD_2Cl_2 δ = 5.62 ppm as internal reference) δ 7.25 (m, 4H; pyridine-H_{meta}), 7.27 (m, 8H; phenyl-H_{meta}), 7.41 (m, 4H; phenyl-H_{para}), 7.55 (m, 8H; phenyl-H_{ortho}), 8.64 (m, 2H; pyridine-H_{para}), 9.27 ppm (m, 4H; pyridine-H_{ortho}); $^{13}C\{^1H\}$ NMR (75.465 MHz, CD_2Cl_2, 25 °C, CD_2Cl_2 δ = 54.0 ppm as internal reference) δ 97.0 (t, $^1J_{PC}$ = 83.1 Hz; P*C*P), 124.6 (s; pyridine-C_{meta}), 128.6 (d, $^3J_{CP}$ = 12.8 Hz; phenyl-C_{meta}), 131.3 (s; phenyl-C_{para}), 131.5 (d, $^2J_{CP}$ = 12.4 Hz; phenyl-C_{ortho}), 136.7 (d, $^1J_{CP}$ = 76.6 Hz; phenyl-C_{ipso}), 150.5 (s; pyridine-C_{para}), 152.5 ppm (s; pyridine-C_{ortho}); $^{31}P\{^1H\}$ NMR (121.5 MHz, CD_2Cl_2, 25 °C, 85% H_3PO_4 as external standard) δ 22.9 ppm (s).

Synthesis of 6. To a solution of **5** (300 mg, 0.39 mmol) in dichloromethane (10 mL) was added 1 equiv of 9-anthracenecarboxaldehyde (81 mg, 0.39 mmol) at room temperature. ^{31}P NMR spectroscopy showed the reaction was complete in 5 min. After evaporation of the solvent, the compound was purified by column chromatography using CH_2Cl_2/Et_2O as a mixture. **6** was finally recovered as a yellow solid in 95% yield (236 mg). Selected data: ^1H NMR (300 MHz, CD_2Cl_2, 25 °C, CD_2Cl_2 δ = 5.62 ppm as internal reference) δ 6.68 (dt, $^4J_{HP}$ = 3.4 Hz, $^3J_{HH}$ = 8.1 Hz, 4H; phenyl-H_{meta}), 6.92 (m, 4H; phenyl-H_{ortho}), 7.33 (m, 8H; phenyl-H_{para}+$H_{para'}$+$H_{meta'}$), 7.44 (m, 2H; anthracenyl-C_3H), 7.62 (m, 2H; anthracenyl-C_2H), 7.77 (m, 2H; anthracenyl-C_4H), 7.96 (m, 1H; anthracenyl-$C_{10}H$), 8.19 (m, 2H; anthracenyl-C_1H), 8.25 (m, 4H; phenyl-$H_{ortho'}$), 9.09 ppm (dd, $^3J_{HP}$ = 29.4 Hz, $^3J_{HP}$ = 40.0 Hz, 1H; P_2C=C*H*); $^{13}C\{^1H\}$ NMR (75.465 MHz, CD_2Cl_2, 25 °C, CD_2Cl_2 δ = 54.0 ppm as internal reference) δ 125.8 (s; anthracenyl-C_3), 126.2 (s; anthracenyl-C_1), 126.7 (s; anthracenyl-C_2), 127.4 (d, $^3J_{PC}$ = 13.0 Hz; phenyl-C_{meta}), 128.0 (d, $^3J_{PC}$ = 13.0 Hz; phenyl-$C_{meta'}$), 128.5 (s; anthracenyl-C_{10}), 128.7 (dd, $^3J_{PC}$ = 6.9 Hz, $^3J_{PC}$ = 17.8 Hz; anthracenyl-C_9), 128.8 (s; anthracenyl-C_4), 129.0 (s; anthracenyl-C_4CC_{10}), 130.6 (dd, $^3J_{PC}$ = 1.6 Hz, $^1J_{PC}$ = 85.1; phenyl-C_{ipso}), 131.3 (s; anthracenyl-C_1CC_9), 131.4 (d, $^4J_{PC}$ = 3.0 Hz; phenyl-C_{para}), 131.6 (d, $^2J_{PC}$ = 11.2 Hz; phenyl-C_{ortho}), 131.8 (d, $^4J_{PC}$ = 3.1 Hz; phenyl-$C_{para'}$), 132.2 (d, $^1J_{PC}$ = 84.4 Hz; phenyl-$C_{ipso'}$), 134.4 (d, $^2J_{PC}$ = 11.1 Hz; phenyl-$C_{ortho'}$), 139.6 (dd, $^1J_{PC}$ = 50.5 Hz, $^1J_{PC}$ = 59.2 Hz; P*C*P), 158.8 ppm (d, $^2J_{PC}$ = 7.5 Hz; P_2C=*C*); $^{31}P\{^1H\}$ NMR (121.5 MHz, CD_2Cl_2, 25 °C, 85% H_3PO_4 as external standard) δ 41.4 (d, $^2J_{PP}$ = 34.9 Hz), 57.9 ppm (d, $^2J_{PP}$ = 34.9 Hz). Anal. Calcd for $C_{40}H_{30}P_2S_2$: C, 75.45; H, 4.75. Found: C, 75.37; H, 4.61.

Synthesis of 7. To a solution of **5** (300 mg, 0.39 mmol) in dichloromethane (10 mL) was added 1 equiv of 2-furaldehyde (38 mg, 0.39 mmol) at room temperature. ^{31}P NMR spectroscopy showed the reaction was complete in 5 min. After evaporation of the solvent, the compound was purified by column chromatography using CH_2Cl_2/Et_2O as a mixture. **7** was finally recovered as a white solid in 93% yield (191 mg). Selected data: ^1H NMR (300 MHz, $CDCl_3$, 25 °C, $CDCl_3$ δ = 7.26 ppm as internal reference) δ 6.09 (m, 1H; furyl-C_4H), 7.03 (m, 1H; furyl-C_3H), 7.03 (m, 4H; phenyl-H_{meta}), 7.10 (m, 1H; furyl-C_5H), 7.14 (m, 2H; phenyl-H_{para}), 7.15 (dd, $^3J_{HP}$ = 26.9 Hz, $^3J_{HP}$ = 38.1 Hz, 1H; P_2C=C*H*), 7.27 (m, 4H; phenyl-$H_{meta'}$), 7.33 (m, 2H; phenyl-$H_{para'}$), 7.71 (m, 4H; phenyl-H_{ortho}), 7.83 ppm (m, 4H; phenyl-$H_{ortho'}$); $^{13}C\{^1H\}$ NMR (75.465 MHz, $CDCl_3$, 25 °C, $CDCl_3$ δ = 77.0 ppm as internal reference) δ 113.0 (s; furyl-C_4), 122.6 (s; furyl-C_3), 123.7 (dd, $^1J_{PC}$ = 58.0 Hz, $^1J_{PC}$ = 61.8 Hz; P*C*P), 127.3 (d, $^3J_{PC}$ = 13.2 Hz; phenyl-C_{meta}), 128.4 (d, $^3J_{PC}$ = 12.7 Hz; phenyl-$C_{meta'}$), 130.1 (dd, $^1J_{PC}$ = 86.2 Hz, $^3J_{PC}$ = 1.5 Hz; phenyl-C_{ipso}), 130.9 (d, $^4J_{PC}$ = 3.1 Hz; phenyl-C_{para}), 131.2 (d, $^1J_{PC}$ = 85.6 Hz; phenyl-$C_{ipso'}$), 131.5 (d, $^4J_{PC}$ = 2.9 Hz; phenyl-$C_{para'}$), 132.4 (d, $^2J_{PC}$ = 10.8 Hz; phenyl-$C_{ortho'}$), 133.4 (d, $^2J_{PC}$ = 11.4 Hz; phenyl-C_{ortho}), 141.2 (d, $^2J_{PC}$ = 8.7 Hz; P_2C=*C*), 145.7 (s; furyl-C_5), 148.8 ppm (dd, $^3J_{PC}$ = 21.9 Hz, $^3J_{PC}$ = 8.1 Hz; furyl-C_2); $^{31}P\{^1H\}$ NMR (121.5 MHz, $CDCl_3$, 25 °C, 85% H_3PO_4 as external standard) δ 39.8 (d, $^2J_{PP}$ = 29.5 Hz), 52.4 ppm (d, $^2J_{PP}$ = 29.5 Hz). Anal. Calcd for $C_{30}H_{24}OP_2S_2$: C, 68.43; H, 4.59. Found: C, 68.27; H 4.65.

Synthesis of 8. To a solution of **5** (300 mg, 0.39 mmol) in dichloromethane (10 mL) was added an excess of benzophenone (360 mg, 2.0 mmol) at room temperature. The resulting solution was stirred for 4 days at 50 °C. ^{31}P NMR spectroscopy showed the reaction was complete. After evaporation of the solvent, the compound was purified by column chromatography using CH_2Cl_2/Et_2O as a mixture. **8** was finally recovered as a white solid in 98% yield (234 mg). Selected data can be found in ref 10.

Synthesis of 9. To a solution of **5** (300 mg, 0.39 mmol) in dichloromethane (10 mL) was added 2.5 equiv of di(2-pyridyl) ketone (180 mg, 0.98 mmol) at room temperature. ^{31}P NMR spectroscopy showed the reaction was complete in 5 min. After evaporation of the solvent, the compound was purified by column chromatography using CH_2Cl_2/Et_2O as a mixture. **9** was finally recovered as a white solid in 96% yield (230 mg). Selected data: ^1H NMR (300 MHz, $CDCl_3$, 25 °C, $CDCl_3$ δ = 7.26 ppm as internal reference) δ 6.88 (m, 2H; pyridyl-C_5H), 7.15 (m, 12H; phenyl-H_{meta} + H_{para}), 7.56 (m, 2H; pyridyl-C_4H), 7.91 (m, 10H; phenyl-H_{ortho} + pyridyl-C_3H), 8.38 ppm (m, 2H; pyridyl-C_6H); $^{13}C\{^1H\}$ NMR (75.465 MHz, $CDCl_3$, 25 °C, $CDCl_3$ δ = 77.0 ppm as internal reference) δ 123.4 (s; pyridyl-C_3), 127.7 (AXX′, $\sum J_{PC}$ = 12.8 Hz; phenyl-C_{meta}), 128.5 (s; pyridyl-C_5), C_{ipso}: not observed, 130.6 (s; phenyl-C_{para}), 131.5 (t, $^1J_{PC}$ = 45.5 Hz; P*C*P), 132.4 (AXX′, $\sum J_{PC}$ = 9.2 Hz; phenyl-C_{ortho}), 136.7 (s; pyridyl-C_2), 147.1 (s; pyridyl-C_6), 154.9 (bs; pyridyl-C_2), 192.5 ppm (bs; P_2C=*C*); $^{31}P\{^1H\}$ NMR (121.5 MHz, $CDCl_3$, 25 °C, 85% H_3PO_4 as external standard) δ 41.5 ppm (s). Anal. Calcd for $C_{36}H_{28}N_2P_2S_2$: C, 70.34; H, 4.59. Found: C, 70.19; H, 4.67.

Synthesis of 10. To a solution of **5** (300 mg, 0.39 mmol) in dichloromethane (10 mL) was added an excess of di(2-thienyl) ketone (390 mg, 2.0 mmol) at room temperature. The resulting solution was stirred for 2 days at 50 °C. ^{31}P NMR spectroscopy showed the reaction was complete. After evaporation of the solvent, the compound was purified by column chromatography using CH_2Cl_2/Et_2O as a mixture. **10** was finally recovered as a white solid in 98% yield (238 mg). Selected data: ^1H NMR (300 MHz, $CDCl_3$, 25 °C, $CDCl_3$ δ = 7.26 ppm as internal reference) δ 6.79 (m, 2H; thienyl-C_4H), 7.13 (m, 10H; phenyl-H_{meta} + thienyl-C_5H), 7.21 (m, 4H; phenyl-H_{para}), 7.94 (m, 8H; phenyl-H_{ortho}), 8.48 ppm (m, 2H; thienyl-C_3H); $^{13}C\{^1H\}$ NMR (75.465 MHz, $CDCl_3$, 25 °C, $CDCl_3$ δ = 77.0 ppm as internal reference) δ 125.3 (s; thienyl-C_4), 127.5 (AXX′, $\sum J_{PC}$ = 12.5 Hz; phenyl-C_{meta}), C_{ipso}: not observed, 130.4 (s; phenyl-C_{para}), 130.8 (t, $^1J_{PC}$ = 57.1 Hz; P*C*P), 132.5 (bs; phenyl-C_{ortho}), 133.1 (s; thienyl-C_5), 135.6 (s; thienyl-C_3), 144.7 (AXX′, $\sum J_{PC}$ = 25.2 Hz; thienyl-C_2), 160.7 ppm (t, $^2J_{PC}$ = 3.1 Hz; P_2C=*C*); $^{31}P\{^1H\}$ NMR (121.5 MHz, $CDCl_3$, 25 °C, 85% H_3PO_4 as external standard) δ 42.0 ppm (s). Anal. Calcd for $C_{34}H_{26}P_2S_4$: C, 65.36; H, 4.19; Found: C, 65.06; H, 4.27.

X-ray Structure Data. Nonius KappaCCD diffractometer, ϕ and ω scans, Mo Kα radiation (λ = 0.71073 Å), graphite monochromator, T = 150 K, structure solution with SIR97,[35] refinement

against F^2 in SHELXL97[36] with anisotropic thermal parameters for all non-hydrogen atoms, calculated hydrogen positions with riding isotropic thermal parameters.

Crystallographic data for the structures reported in this paper have been deposited with the Cambridge Crystallographic Data Centre as supplementary publications no. CCDC-616091 (**2**), CCDC-616092 (**4**), and CCDC-616093 (**5**). Copies of the data can be obtained free of charge on application to CCDC, 12 Union Road, Cambridge CB21EZ, UK (fax: (+44) 1223-336-033; e-mail: deposit@ccdc.cam.ac.uk).

Computational Details. All calculations were carried out using the Gaussian 03W package.[27] Geometry optimizations were carried out at the B3LYP[37] level of theory, which is a hybrid functional consisting of Becke's exchange,[38] Slater's exchange,[39−41] exact Hartree−Fock exchange, VWN correlation,[42] and the nonlocal (gradient) part of the LYP correlation functionals.[43] The basis set LANL2DZ[44] plus an f-type polarization function with an exponent of 0.875 was used for Zr. C, H, N, P, S, and Cl atoms were represented by the 6-31+G* basis set. Electronic structures of these model compounds were studied using natural bond orbital (NBO) analysis, by the mean of the NBO 3.0 program interfaced into the Gaussian program. Compositions of molecular orbitals were calculated using the AOMix program.[28,29]

Acknowledgment. The authors thank the CNRS (Centre National de la Recherche Scientifique) and the Ecole Polytechnique for the financial support of this work and IDRIS for the allowance of computer time (project no. 061616).

Supporting Information Available: CIF files for **2**, **4**, and **5** and optimized geometries and frequencies for **2t**, **2t′**, and **5t**. This material is available free of charge via the Internet at http://pubs.acs.org.

OM060665V

(35) Altomare, A.; Burla, M. C.; Camalli, M.; Cascarano, G. L.; Giacovazzo, C.; Guagliardi, A.; Moliterni, A. G. G.; Polidori, G.; Spagna, R. *J. Appl. Crystallogr.* **1999**, *32*, 115−119.

(36) Sheldrick, G. M. *SHELXL-97*; Universität Göttingen: Göttingen, Germany, 1997.

(37) Becke, A. D. *J. Chem. Phys.* **1993**, *98*, 5648−5652.

(38) Becke, A. D. *Phys. Rev. A* **1988**, *38*, 3098−3100.

(39) Kohn, W.; Sham, L. J. *Phys. Rev.* **1965**, *140*, 1133.

(40) Hohenberg, P.; Kohn, W. *Phys. Rev. B* **1964**, *136*, B864.

(41) Slater, J. C. In *Quantum Theory of Molecular and Solids Vol. 4: The Self-Consistent Field for Molecular and Solids*; McGraw-Hill: New York, 1974.

(42) Vosko, S. H.; Wilk, L.; Nusair, M. *Can. J. Phys.* **1980**, *58*, 1200−1211.

(43) Lee, C. T.; Yang, W. T.; Parr, R. G. *Phys. Rev. B* **1988**, *37*, 785−789.

(44) Hay, P. J.; Wadt, W. R. *J. Chem. Phys.* **1985**, *82*, 299−310.